

Approximate Exponential Integrators for Time-Dependent Equation-of-Motion Coupled Cluster Theory

David B. Williams-Young,^{*,†} Stephen H. Yuwono,[‡] A. Eugene DePrince, III,[‡]
and Chao Yang[†]

[†]*Applied Mathematics and Computational Research Division, Lawrence Berkeley National
Laboratory, Berkeley, CA*

[‡]*Department of Chemistry and Biochemistry, Florida State University, Tallahassee, FL*

E-mail: dbwy@lbl.gov

Abstract

With growing demand for time-domain simulations of correlated many-body systems, the development of efficient and stable integration schemes for the time-dependent Schrödinger equation is of keen interest in modern electronic structure theory. In the present work, we present two novel approaches for the formation of the quantum propagator for time-dependent equation-of-motion coupled cluster theory (TD-EOM-CC) based on the Chebyshev and Arnoldi expansions of the complex, non-hermitian matrix exponential, respectively. The proposed algorithms are compared with the short-iterative Lanczos method of Cooper, *et al* [*J. Phys. Chem. A* **2021** 125, 5438-5447], the fourth-order Runge-Kutta method (RK4), and exact dynamics for a set of small but challenging test problems. For each of the cases studied, both of the proposed integration schemes demonstrate superior accuracy and efficiency relative to the reference simulations.

1 Introduction

In recent years, there has been renewed interest in the development of efficient numerical methods to study the quantum dynamics of correlated electrons in molecular and materials systems (see, e.g., Refs. 1,2 and references therein). Under particular approximations, it is possible to circumvent the direct solution of the time-dependent Schrödinger equation (TDSE) in favor of time-dependent perturbation theory (or “frequency-domain” methods) which aims to implicitly access quantum dynamics through probing the spectral structure of the Hamiltonian operator. In the context of electronic structure theory, these approaches include linear-response,³⁻⁵ polarization propagator,⁶⁻⁸ and equation-of-motion⁹⁻¹² methods among others.¹³⁻¹⁵ While these methods can often be a powerful tool for the simulation and prediction of observable phenomena such as spectroscopies, their veracity depends on the applicability of their various approximations to accurately characterize queried physical conditions. Further, the vast majority of these perturbative methods serve to access the *equilibrium* behaviour of electronic dynamics, leaving non-equilibrium phenomena, such as charge migration,¹⁶ inaccessible. From a theoretical perspective, time-domain simulations do not suffer from these deficiencies and may be straightforwardly extended to non-perturbative and non-equilibrium regimes.^{1,2}

Given the ability to faithfully represent physical conditions by a chosen Hamiltonian, wave-function ansatz, and initial condition, the primary challenges of time-domain electronic structure methods are practical rather than theoretical. In contrast to frequency-domain methods which trade the problem of temporal dynamics for the tools of numerical linear algebra,¹⁷⁻²² time-domain methods require explicit integration of the TDSE, which is generally more resource intensive. For hermitian discretizations of molecular Hamiltonians, such as Hartree-Fock (real-time time-dependent HF, RT-TDHF^{23,24}), density functional theory (RT-TDDFT),²⁵ and configuration interaction (TD-CI),²⁶⁻²⁹ significant research effort has been afforded to the development of efficient numerical methods to integrate the TDSE.^{30,31} In particular, approximate exponential integrators based on polynomial (Chebyshev^{30,32-35})

and Krylov subspace (short-iterative Lanczos,³⁶ SIL) expansions of the quantum propagator are among the most widely used integration techniques for hermitian quantum dynamics. Exponential integrators are powerful geometric techniques for the solution of linear ordinary differential equations (ODE), such as the TDSE, as they preserve their exact flow,³⁷ thereby allowing for much larger time-steps than simpler, non-geometric integrators such as the fourth-order Runge-Kutta method (RK4). In addition, these methods may also be formulated in such a way as to only require knowledge of the action of a matrix-vector product,^{30,38–40} thereby avoiding explicit materialization of the Hamiltonian matrix which is generally large for correlated many-body wave-functions.

The situation is significantly more complex for non-hermitian Hamiltonian discretizations such as those arising from coupled-cluster (CC) theory (see Ref. 41 for a recent review). Due to its simplicity and low memory requirement, RK4 is generally the integrator of choice for time-domain CC methods in the recent past.⁴¹ Symplectic,^{42–44} multistep,⁴⁵ and adaptive⁴⁶ integrators for time-domain CC methods have been developed, and have yielded significant efficiency improvements over their non-symplectic counterparts. Exponential Runge-Kutta integrators have been explored in the context of nonlinear time-dependent CC theory (TD-CC),⁴⁷ but have yet to see wider adoption. Recently, Cooper, *et al.*⁴⁸ suggested an approximate exponential integration scheme for time-dependent equation-of-motion CC theory (TD-EOM-CC)^{29,41,43,49–52} based on the hermitian SIL method to efficiently generate linear absorption spectra for molecular systems. Despite being only valid for hermitian matrices, the proposed SIL approach was demonstrated to produce sufficiently accurate spectra with relatively low subspace dimensions. However, the ability of this scheme to produce faithful, long-time dynamics within TD-EOM-CC has not been assessed, and is unlikely due to its hermitian ill-formation. In this work, we pursue the development and assessment of polynomial and non-hermitian Krylov subspace (short-iterative *Arnoldi*, SIA) methods for the complex matrix exponential to enable the efficient and accurate simulation of TD-EOM-CC.

The remainder of this work is organized as follows. In Sec. 2.1, we review the salient

aspects of TD-EOM-CC theory relevant to the development of efficient exponential integrators. In Secs. 2.2 and 2.3 we examine the properties of exact and approximate dynamics for the TD-EOM-CC ODE and present the developed integration schemes based on the Chebyshev (Sec. 2.3.1) and SIA (Sec. 2.3.2) expansions of the complex matrix exponential. In Sec. 3, we apply the developed integration schemes to a set of small test problems and compare their veracity with exact dynamics as well as previously employed SIL and RK4 methods. We conclude this work in Sec. 4 and offer outlook on future directions for approximate exponential integrator development in TD-EOM-CC in the years to come.

2 Theory and Methods

2.1 Time-Dependent Equation-of-Motion Coupled-Cluster Theory

Time-dependent equation-of-motion coupled-cluster (TD-EOM-CC) theory is a general time-domain reformulation of many-body quantum mechanics capable of simulating the dynamics of both time-dependent^{29,41,49,50} and time-independent^{51,52} Hamiltonians. In this work, we consider the moment-based formulation⁵¹ of TD-EOM-CC to compute the spectral function,

$$f(\omega) = \frac{2}{3}\omega \int_{-\infty}^{\infty} dt e^{-i\omega t} S(t), \quad (1)$$

where $S(t) = \langle \tilde{M}(0) | M(-t) \rangle = \langle \tilde{M}(t) | M(0) \rangle$ is the autocorrelation function. Here, $|M(t)\rangle$ ($\langle \tilde{M}(t) |$) is (the dual of) the time-dependent moment function which describes the propagation of weak perturbations throughout the many-body system. We note for clarity that, due to the nonhermiticity of the CC formalism, $\langle \tilde{M}(t) |$ is not the complex conjugate of $|M(t)\rangle$. Additionally, throughout this paper, we chose $S(t)$ to be $\langle \tilde{M}(0) | M(-t) \rangle$, although $\langle \tilde{M}(t) | M(0) \rangle$ is also valid. $|M(t)\rangle$ ($\langle \tilde{M}(t) |$) may generally be described via a linear expansion

of (de-)excitations from a reference state $|0\rangle$ (typically taken to be HF),

$$|M(t)\rangle = \left(m_0(t) + \sum_{ai} m_i^a(t) c_a^\dagger c_i + \frac{1}{4} \sum_{abij} m_{ij}^{ab}(t) c_a^\dagger c_b^\dagger c_j c_i + \dots \right) |0\rangle \quad (2)$$

$$\langle \tilde{M}(t)| = \langle 0| \left(\tilde{m}_0(t) + \sum_{ai} \tilde{m}_a^i(t) c_i^\dagger c_a + \frac{1}{4} \sum_{abij} \tilde{m}_{ab}^{ij}(t) c_i^\dagger c_j^\dagger c_b c_a + \dots \right) \quad (3)$$

where m_0 (\tilde{m}_0), m_i^a (\tilde{m}_a^i) and m_{ij}^{ab} (\tilde{m}_{ab}^{ij}) are time-dependent (de-)excitation amplitudes, c_p (c_p^\dagger) is the fermionic annihilation (creation) operator associated with the spin-orbital p , and the indices i, j, \dots and a, b, \dots denote occupied and virtual spin-orbitals relative to $|0\rangle$. In this work, we truncate Eq. (2) to only include up to double excitations from the reference, resulting in the TD-EOM-CCSD approach.

Within the TD-EOM-CC formalism, the moment excitation and de-excitation amplitudes obey the following set of coupled, linear-time-invariant (LTI) ODEs⁵¹

$$\partial_t \mathbf{m}(t) = -i \overline{\mathbf{H}}_N \mathbf{m}(t), \quad \mathbf{m}(t) = \begin{bmatrix} m_0(t) \\ \{m_i^a(t)\} \\ \{m_{ij}^{ab}(t)\} \end{bmatrix} \in \mathbb{C}^n, \quad (4)$$

and their left-hand counterparts

$$\partial_t \tilde{\mathbf{m}}(t) = i \overline{\mathbf{H}}_N^T \tilde{\mathbf{m}}(t), \quad \tilde{\mathbf{m}}(t) = \begin{bmatrix} \tilde{m}_0(t) \\ \{\tilde{m}_i^a(t)\} \\ \{\tilde{m}_{ij}^{ab}(t)\} \end{bmatrix} \in \mathbb{C}^n, \quad (5)$$

where $\overline{\mathbf{H}}_N \in \mathbb{C}^{n \times n}$ is the non-hermitian, normal-ordered, similarity-transformed Hamiltonian represented in the basis of Slater determinants.^{10,11} From the moment state-vectors, $\mathbf{m}(t)$ and $\tilde{\mathbf{m}}(t)$, $S(t)$ of Eq. (1) may be evaluated as

$$S(t) = \tilde{\mathbf{m}}^T \mathbf{m}(-t), \quad (6)$$

where we have taken $\tilde{\mathbf{m}} \equiv \tilde{\mathbf{m}}(0)$. It is worth mentioning that the TD-EOM-CCSD formalism used here requires propagating only the right- or left-hand moment amplitudes [in this case, the right-hand amplitudes following Eq. (4)]. While Eq. (1) is perturbatively derived from Fermi's Golden Rule,⁵¹ time evolution of $|M(t)\rangle$ via Eq. (4) also serves as a useful model for the development of both LTI and non-LTI integration techniques for TD-EOM-CC methods as it formally consists of the same algorithmic components that are required for the simulation of time-dependent Hamiltonians.^{29,41,49,50}

When specified as an initial value problem, Eq. (4) admits an analytic solution

$$\mathbf{m}(t) = \exp(-i\overline{\mathbf{H}}_N t) \mathbf{m}(0) \quad (7)$$

where $\exp(-i\overline{\mathbf{H}}_N t)$ is the quantum propagator and \exp is the matrix exponential defined in the canonical way.⁵³ We refer the reader to Refs. 51,52 for discussions pertaining to the choices of initial conditions for Eq. (7) to simulate various spectroscopic properties. In this work, we consider the dipole initial conditions⁵¹ induced by

$$|M(0)\rangle = \bar{\mu}|0\rangle, \quad \langle \tilde{M}(0)| = \langle 0|(1 + \hat{\Lambda})\bar{\mu}, \quad \bar{\mu} = \exp(-\hat{T}) \hat{\mu} \exp(\hat{T}), \quad (8)$$

where \hat{T} and $\hat{\Lambda}$ are the ground-state CC excitation and de-excitation operators (again truncated at double excitation/de-excitations in this work), and $\hat{\mu}$ is a particular component of the electronic dipole operator.

2.2 Exact Matrix Exponential

When $\overline{\mathbf{H}}_N$ is small enough to be formed explicitly in memory, Eq. (7) may be directly evaluated as

$$\mathbf{m}^{\text{ex}}(t) = \mathbf{R} \exp(-i\Omega t) \mathbf{w}^{\text{ex}}, \quad \mathbf{w}^{\text{ex}} = \mathbf{L} \mathbf{m}(0) \quad (9)$$

where $\mathbf{\Omega} \in \mathbb{C}^{n \times n}$ is the diagonal matrix of EOM-CC eigenvalues, $\mathbf{\Omega} = \{\omega_I \in \mathbb{C}\}_{I=1}^n$, and $\mathbf{L}, \mathbf{R} \in \mathbb{C}^{n \times n}$ are the full, biorthogonal set of corresponding left and right eigenvectors satisfying the equations^{10,11}

$$\overline{\mathbf{H}}_N \mathbf{R} = \mathbf{R} \mathbf{\Omega}, \quad \mathbf{L} \overline{\mathbf{H}}_N = \mathbf{\Omega} \mathbf{L}, \quad \mathbf{L} \mathbf{R} = \mathbf{I} \quad (10)$$

where $\mathbf{I} \in \mathbb{C}^{n \times n}$ is the identity-matrix. As $\mathbf{\Omega}$ is a diagonal matrix, $\exp(-i\mathbf{\Omega}t)$ is simply the diagonal matrix with entries $e^{-i\omega_I t}$. Insertion of Eq. (9) into Eq. (6) yields the following simple expression for the exact autocorrelation function

$$S_{\text{ex}}(t) = \tilde{\mathbf{w}}^{\text{ex},\text{T}} \exp(i\mathbf{\Omega}t) \mathbf{w}^{\text{ex}}, \quad \tilde{\mathbf{w}}^{\text{ex}} = \mathbf{R}^{\text{T}} \tilde{\mathbf{m}}. \quad (11)$$

As a non-hermitian matrix, $\overline{\mathbf{H}}_N$ is not guaranteed to have real eigenvalues if the many-electron basis is truncated, and as such, Eq. (9) (and by extension Eq. (7)) is not guaranteed to be unitary (norm-preserving) and will generally yield dissipative or divergent dynamics along EOM-CC modes with $\Im\omega_I \neq 0$ (see, *e.g.*, a recent study in Ref. 54). However, it has been shown that,^{55,56} barring suboptimal ground-state CC solutions or the presence of conical intersections, $\overline{\mathbf{H}}_N$ typically admits a real spectrum representing physical excited states and thus, Eq. (9) is unitary in exact arithmetic.

2.3 Approximate Exponential Integrators

While Eq. (9) is an exact solution to the LTI TD-EOM-CC dynamics considered in this work, it requires the full diagonalization of $\overline{\mathbf{H}}_N$. As the memory requirement associated with the EOM-CCSD $\overline{\mathbf{H}}_N$ grows $O(N^8)$ with system size, full diagonalization is impractical for all but the smallest problems. For some systems, it is possible to integrate the TD-EOM-CC equations in a subspace spanned by a small number of states such that full diagonalization is not required.^{29,41,49,50} However, if a large number of states are required or spectral regions of interest are densely populated or spectrally interior, this approach also becomes impractical.

Matrix exponentiation is a challenging numerical linear algebra problem, and the past half century has yielded a wealth of research into the development of efficient implicit^{30,38–40} and direct⁵³ methods both for hermitian and non-hermitian matrices. In this work, we will consider subspace approaches for evaluation of the complex, non-hermitian matrix exponential generally taking the form

$$\mathbf{m}(t + \delta t) = \exp(-i\overline{\mathbf{H}}_N\delta t) \mathbf{m}(t) \approx \mathbf{V}\mathbf{c}(\delta t), \quad (12)$$

where $\mathbf{V} \in \mathbb{C}^{n \times k}$ is a k -dimensional subspace (with $k \ll n$) generated by the action of $-i\overline{\mathbf{H}}_N$ onto the current state vector, $\mathbf{m}(t)$, and $\mathbf{c}(\delta t) \in \mathbb{C}^k$ is a time-varying coefficient vector. Given the ability to implicitly form $\boldsymbol{\sigma} \leftarrow \overline{\mathbf{H}}_N\mathbf{v}$ (i.e. a “ σ build”), which is a standard algorithmic component of any EOM-CC implementation,^{10,11} the implementations of Eq. (12) considered in this work will not require materialization of $\overline{\mathbf{H}}_N$ in memory. Within the subspace ansatz, Eq. (6) becomes

$$S(t + \delta t) \approx \tilde{\mathbf{w}}^T \mathbf{c}(-\delta t), \quad \tilde{\mathbf{w}} = \mathbf{V}^T \tilde{\mathbf{m}} \in \mathbb{C}^k, \quad (13)$$

where $\tilde{\mathbf{w}}$ is time-independent for fixed \mathbf{V} .

For a particular expansion order k and state vector $\mathbf{m}(t)$, Eq. (12) will generally be valid for $|\delta t| \leq |\Delta t|$, where Δt will be referred to as a *macro time-step* in the following. Within this prescription, the total simulation length, \mathcal{T} , will be partitioned into subintervals $\{\mathcal{T}_i = [t_i, t_{i+1}]\}$ where $t_0 = 0$, $t_i = t_{i-1} + \Delta t_i$, and Δt_i is the macro time step for the i -th interval. The relationship between k and Δt is method-dependent, and will be discussed for both the Chebyshev and Arnoldi integrators below. Due to the factorization of the time-dependence into $\mathbf{c}(t)$, a general property of truncated expansions such as Eq. (12) is in their ability to interpolate within each \mathcal{T}_i without requiring additional σ builds.³⁰ This property is particularly advantageous for methods such as EOM-CCSD in which the computational complexity of σ formation scales $O(N^6)$ with system size.^{10,11} For each \mathcal{T}_i , a single \mathbf{V} is computed and the propagator may be interpolated to arbitrary temporal

resolution by varying the corresponding coefficients. For each of the intermediate time intervals ($i > 0$), the approximation of $\mathbf{m}(t_{i+1})$ generated from the endpoint of \mathcal{T}_i is used as the starting vector to generate \mathbf{V} for \mathcal{T}_{i+1} .

2.3.1 Chebyshev Time Integration

The use of the Chebyshev expansion to evaluate the quantum propagator for hermitian Hamiltonians is well established and is among the most efficient known strategies for integrating LTI variants of the TDSE.^{30,32-35} In this work, we demonstrate that this approach is also applicable to non-hermitian Hamiltonians with real spectra. Chebyshev polynomials of the first kind, $\{\Phi_p\}$, given by the recurrence

$$\Phi_0(z) = 1, \quad \Phi_1(z) = z, \quad \Phi_{p+1}(z) = 2z\Phi_p(z) - \Phi_{p-1}(z), \quad (14)$$

are a powerful tool in the approximation of scalar and matrix functions on the real-line as they form the unique approximation basis which minimizes the uniform (infinity) norm on $[-1, 1]$ at a particular order.⁵⁷ In the Chebyshev basis, the TD-EOM-CC propagator acting on a general vector \mathbf{v} may be exactly expanded as^{30,32}

$$\exp(-i\overline{\mathbf{H}}_N\delta t)\mathbf{v} = e^{-i\gamma_+\delta t} \sum_{p=0}^{\infty} (2 - \delta_{p0}) J_p(\gamma_-\delta t) \Phi_p(-i\tilde{\mathbf{H}}_N)\mathbf{v} \quad (15)$$

where $\gamma_{\pm} = \frac{1}{2}(\omega_{\max} \pm \omega_{\min})$, $\omega_{\min/\max}$ are the minimum/maximum eigenvalues of $\overline{\mathbf{H}}_N$, δ_{k0} is a Kronecker delta, J_p is the p -th Bessel function of the first kind, and $\tilde{\mathbf{H}}_N = \gamma_-^{-1}(\overline{\mathbf{H}}_N - \gamma_+\mathbf{I})$ is an auxiliary matrix that scales the spectrum of $\overline{\mathbf{H}}_N$ from $[\omega_{\min}, \omega_{\max}] \rightarrow [-1, 1]$ such that the image of Φ_p remains on the unit disk. Practically, $\tilde{\mathbf{H}}_N$ need not be formed explicitly (see Alg. 1) and γ_{\pm} need not be computed from exact eigenvalues and can be approximated using standard techniques⁵⁸⁻⁶² as long as the mapped spectral bounds are contained in $[-1, 1]$.

In practice, the sum in Eq. (15) is truncated to a finite order k , yielding a compact representation of the propagator in the Chebyshev basis, $\mathbf{V}_{\text{cheb}} = [\mathbf{v}_0^{\text{cheb}}, \mathbf{v}_1^{\text{cheb}}, \mathbf{v}_2^{\text{cheb}}, \dots, \mathbf{v}_{k-1}^{\text{cheb}}]$,

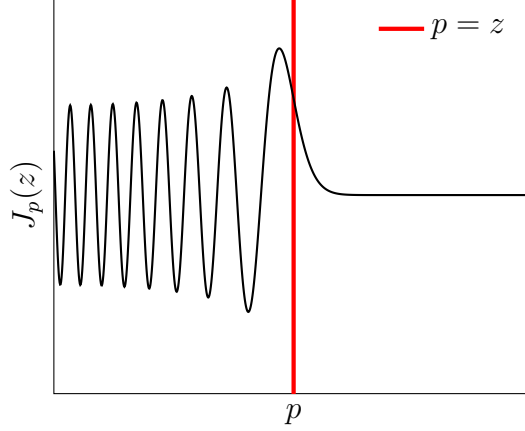


Figure 1: Graphical depiction of the order decay behaviour of Bessel functions of the first kind for fixed argument. The function is highly oscillatory for $p < z$ but decays exponentially for $p > z$.

given by

$$\mathbf{v}_p^{\text{cheb}} = \Phi_p(-i\tilde{\mathbf{H}}_N)\mathbf{m}(t), \quad c_p^{\text{cheb}}(\delta t) = e^{-i\gamma+\delta t}(2 - \delta_{p0})J_p(\gamma-\delta t). \quad (16)$$

The truncation error at the interval endpoint $(t + \Delta t)$ of the Chebyshev expansion can be shown^{63,64} to be bounded by

$$C(\Delta t) = 2\|\mathbf{v}\| \sum_{p=k}^{\infty} |J_p(\gamma-\Delta t)|. \quad (17)$$

For fixed argument, $J_p(z)$ is highly oscillatory for $p < z$ but decays exponentially for $p > z$, as depicted in Fig. 1. We note that for even (odd) p , J_p is an even (odd) function about zero. Therefore, for p sufficiently larger than $|\gamma-\Delta t|$, we may approximate $C(\Delta t) \approx 2\|\mathbf{v}\||J_p(\gamma-\Delta t)|$. Given a desired step size, Δt_{cheb} , and error threshold $\varepsilon^{\text{cheb}}$, we may use this approximation to select $k > |\gamma-\Delta t_{\text{cheb}}|$ such that $|J_k(\gamma-\Delta t_{\text{cheb}})| < \frac{\varepsilon^{\text{cheb}}}{2\|\mathbf{v}\|}$.

As Δt_{cheb} is fixed, \mathcal{T} may be evenly partitioned into $\lceil \frac{\mathcal{T}}{|\Delta t_{\text{cheb}}|} \rceil$ intervals. The Chebyshev subspace vectors may be efficiently evaluated using only k σ -builds (Alg. 1), thus the total σ -build cost for this method is $\lceil \frac{\mathcal{T}}{|\Delta t_{\text{cheb}}|} \rceil \cdot k$. Another important aspect of the Chebyshev method is that, due to fact that the expressions in Eq. (16) are analytic, one need not materialize \mathbf{V}_{cheb} in memory. Instead, one may evaluate $\tilde{\mathbf{w}}^{\text{cheb}} = \mathbf{V}_{\text{cheb}}^{\text{T}}\tilde{\mathbf{m}}$ (Eq. (13)) directly as the

Algorithm 1: Evaluation of Eqs. (13) and (15) via the Chebyshev Expansion

Input: $\overline{\mathbf{H}}_N \in \mathbb{C}^{n \times n}$, $\gamma_{\pm} \in \mathbb{R}$, $\Delta t_{\text{cheb}} \in \mathbb{R}$, Truncation order $k \in \mathbb{Z}^+$, $\tilde{\mathbf{m}} \in \mathbb{C}^n$, and current state vector $\mathbf{m}(t) \in \mathbb{C}^n$

Returns: $\tilde{\mathbf{w}}^{\text{cheb}}$, $\mathbf{m}_* \approx \mathbf{m}(t + \Delta t_{\text{cheb}})$

```

1  $\alpha \leftarrow \gamma_- \Delta t_{\text{cheb}}$ 
2  $\mathbf{v}_- \leftarrow \mathbf{m}(t)$ 
3  $\tilde{\mathbf{w}}_0^{\text{cheb}} \leftarrow \mathbf{v}_-^T \tilde{\mathbf{m}}$ 
4  $\mathbf{m}_* \leftarrow J_0(\alpha) \mathbf{v}_-$ 
5  $\boldsymbol{\sigma} \leftarrow \overline{\mathbf{H}}_N \mathbf{v}_-$ 
6  $\mathbf{v}_0 \leftarrow -i\gamma_-^{-1} (\boldsymbol{\sigma} - \gamma_+ \mathbf{v}_-)$ 
7  $\tilde{\mathbf{w}}_1^{\text{cheb}} \leftarrow \mathbf{v}_0^T \tilde{\mathbf{m}}$ 
8  $\mathbf{m}_* \leftarrow \mathbf{m}_* + 2J_1(\alpha) \mathbf{v}_0$ 
   for  $p \in [2, k)$  do
9      $\boldsymbol{\sigma} \leftarrow \overline{\mathbf{H}}_N \mathbf{v}_0$ 
10     $\mathbf{v}_+ \leftarrow -2i\gamma_-^{-1} (\boldsymbol{\sigma} - \gamma_+ \mathbf{v}_0) + \mathbf{v}_-$ 
11     $\tilde{\mathbf{w}}_p^{\text{cheb}} \leftarrow \mathbf{v}_+^T \tilde{\mathbf{m}}$ 
12     $\mathbf{m}_* \leftarrow \mathbf{m}_* + 2J_p(\alpha) \mathbf{v}_+$ 
13     $\mathbf{v}_- \leftarrow \mathbf{v}_0$ 
14     $\mathbf{v}_0 \leftarrow \mathbf{v}_+$ 
   end
15  $\mathbf{m}_* \leftarrow e^{-\gamma_+ \Delta t_{\text{cheb}}} \mathbf{m}_*$ 

```

subspace is generated, as is shown in Alg. 1, thus changing the memory requirement from $O(kn)$ to $O(3n)$. As it is often the case that one requires high-order Chebyshev polynomials ($\gg 3$) to accurately approximate the matrix exponential, this realization leads to a drastic reduction in memory consumption for large systems.

2.3.2 Short Iterative Arnoldi Time Integration

Considering the spectral decomposition of the exact propagator given in Sec. 2.2, it is expected that the Chebyshev method discussed in Sec. 2.3.1 will be most effective when Ω is nearly uniformly distributed within $[\omega_{\min}, \omega_{\max}]$, due to the fact that the Chebyshev basis minimizes the uniform function norm. If Ω is clustered, Krylov subspace techniques for the formation of the exponential propagator are often more effective.³⁸ The basic principle behind Krylov approximation techniques for matrix-functions is rooted in the generation of a

k -dimensional, orthonormal basis, $\mathbf{V}_{\text{krlv}} = [\mathbf{v}_0^{\text{krlv}}, \mathbf{v}_1^{\text{krlv}}, \dots, \mathbf{v}_{k-1}^{\text{krlv}}]$, for the Krylov subspace

$$\mathcal{K}^k(\overline{\mathbf{H}}_N, \mathbf{v}_0) = \{\mathbf{v}_0, \overline{\mathbf{H}}_N \mathbf{v}_0, \overline{\mathbf{H}}_N^2 \mathbf{v}_0, \dots, \overline{\mathbf{H}}_N^{k-1} \mathbf{v}_0\}. \quad (18)$$

where $\mathbf{v}_0 \in \mathbb{C}^n$ is an arbitrary vector with $\|\mathbf{v}_0\| = 1$. Given \mathbf{V}_{krlv} , one may form a subspace-projected Hamiltonian,

$$\mathbf{H}_{\text{krlv}} = \mathbf{V}_{\text{krlv}}^\dagger \overline{\mathbf{H}}_N \mathbf{V}_{\text{krlv}} \in \mathbb{C}^{k \times k} \quad (19)$$

and approximate the action of the matrix exponential as³⁸

$$\exp(-i\overline{\mathbf{H}}_N \delta t) \mathbf{v} \approx \mathbf{V}_{\text{krlv}} \mathbf{c}_{\text{krlv}}(\delta t), \quad \mathbf{c}_{\text{krlv}}(\delta t) = \|\mathbf{v}\| \exp(-i\mathbf{H}_{\text{krlv}} \delta t) \mathbf{e}_1, \quad (20)$$

where \mathbf{e}_1 is the first column of a $k \times k$ identity matrix and \mathbf{V}_{krlv} is the Krylov subspace generated from $\mathbf{v}_0 = \mathbf{v}/\|\mathbf{v}\|$. Given that $k \ll n$, the exponential in Eq. (20) may be efficiently evaluated via Eq. (9).

For hermitian matrices, \mathbf{V}_{krlv} can be efficiently generated by the Lanczos iteration,⁶⁵ \mathbf{H}_{krlv} is a tridiagonal matrix, and both \mathbf{H}_{krlv} and \mathbf{V}_{krlv} may be formed implicitly via a simple three-term recursion. For the approximation of the propagator, this approach has come to be known as the short-iterative Lanczos (SIL) method.³⁶ Here, we present an analogous scheme for the exponential propagator based on the Arnoldi iteration,^{65,66} which is a general Krylov subspace technique which extends to both hermitian and non-hermitian matrices. We will refer to this approach as the short-iterative Arnoldi (SIA) method in the following. Instead of a tridiagonal matrix, the Arnoldi method produces an upper Hessenberg matrix via the recursion

$$\overline{\mathbf{H}}_N \mathbf{V}_{\text{krlv}} = \mathbf{V}_{\text{krlv}} \mathbf{H}_{\text{krlv}} + \beta_{k+1} \mathbf{v}_{k+1}^{\text{krlv}} \mathbf{e}_k^T \quad (21)$$

where \mathbf{e}_k is the k -th column of the $k \times k$ identity matrix and $\beta_{k+1} \mathbf{v}_{k+1}^{\text{krlv}}$ is the residual

$$\beta_{k+1} \mathbf{v}_{k+1}^{\text{krlv}} = (\mathbf{I} - \mathbf{V}_{\text{krlv}} \mathbf{V}_{\text{krlv}}^\dagger) \overline{\mathbf{H}}_N \mathbf{v}_k^{\text{krlv}}, \quad (22)$$

Algorithm 2: The Arnoldi Iteration

Input: $\overline{\mathbf{H}}_N \in \mathbb{C}^{n \times n}$, $\mathbf{v}_0 \in \mathbb{C}^n$ with $\|\mathbf{v}_0\|_2 = 1$, Krylov dimension $k \in \mathbb{Z}^+$
Returns: Krylov basis $\mathbf{V}_k \in \mathbb{C}^{n \times k}$, Projected Hamiltonian $\mathbf{H}_{\text{krlv}} \in \mathbb{C}^{k \times k}$.

```

1  $\mathbf{v}_0^{\text{krlv}} \leftarrow \mathbf{v}_0$ 
2  $\mathbf{V}_{\text{krlv}} \leftarrow [\mathbf{v}_0^{\text{krlv}}]$ 
  for  $p \in [0, k - 1)$  do
3    $\boldsymbol{\sigma} \leftarrow \overline{\mathbf{H}}_N \mathbf{v}_p^{\text{krlv}}$ 
4    $\mathbf{h}_1 \leftarrow \mathbf{V}_{\text{krlv}}^T \boldsymbol{\sigma}$  ; // Classical Gram-Schmidt
5    $\boldsymbol{\sigma} \leftarrow \boldsymbol{\sigma} - \mathbf{V}_{\text{krlv}} \mathbf{h}_1$ 
6    $\mathbf{h}_2 \leftarrow \mathbf{V}_{\text{krlv}}^T \boldsymbol{\sigma}$  ; // Reorthogonalization
7    $\boldsymbol{\sigma} \leftarrow \boldsymbol{\sigma} - \mathbf{V}_{\text{krlv}} \mathbf{h}_2$ 
8    $\beta \leftarrow \|\boldsymbol{\sigma}\|_2$ 
9    $\mathbf{H}_{\text{krlv}}(0 : p, p) \leftarrow \mathbf{h}_1 + \mathbf{h}_2$ 
10   $\mathbf{H}_{\text{krlv}}(p + 1, p) \leftarrow \beta$ 
11   $\mathbf{v}_{p+1}^{\text{krlv}} \leftarrow \beta^{-1} \boldsymbol{\sigma}$ 
12   $\mathbf{V}_{\text{krlv}} \leftarrow [\mathbf{V}_{\text{krlv}}, \mathbf{v}_{p+1}^{\text{krlv}}]$ 
  end

```

with $\|\mathbf{v}_{k+1}^{\text{krlv}}\| = 1$. If $\overline{\mathbf{H}}_N$ were an hermitian matrix, \mathbf{H}_{krlv} would be tridiagonal and \mathbf{V}_{krlv} would span the same subspace as the one produced by the Lanczos iteration in exact arithmetic.

Much like the Lanczos iteration, \mathbf{H}_{krlv} may also be formed incrementally via the Arnoldi iteration as shown in Alg. 2. However, unlike the 3-term recurrence used in the Lanczos method, the Arnoldi iteration requires *explicit* orthogonalization of newly produced subspace vectors as opposed to the implicit orthogonalization generated by Lanczos. As the Arnoldi method is guaranteed to produce orthonormal basis via explicit orthogonalization, it is often more numerically stable even for hermitian problems.^{67–69} In this work, we have utilized the classical Gram-Schmidt method with reorthogonalization to perform the explicit basis orthogonalization.⁷⁰ There exist non-hermitian extensions of the Lanczos method⁷¹ which produce simultaneous, biorthogonal approximations for the left- and right-hand eigenspaces of non-hermitian matrices and have seen successful applications in both frequency domain CC applications¹⁹ as well as in state selection for TD-EOM-CC.⁵⁰ However, the biorthogonalization requirements of these methods can often be numerically unstable,^{72–74} and as such,

we expect the Arnoldi method to yield superior numerical stability in finite precision.⁷⁵

It has been shown³⁸ that the error produced by Eq. (20) can be bounded by the right hand side of the following inequality

$$\|\exp(i\overline{\mathbf{H}}_N\delta t)\mathbf{v}_0 - \mathbf{V}_{\text{kriv}}\exp(i\mathbf{H}_{\text{kriv}}\delta t)e_1\|_2 \leq 2\beta_{k+1}(\delta t\rho)^k \max(1, e^{\mu(-\overline{\mathbf{H}}_N)\delta t}), \quad (23)$$

where $\mu(\overline{\mathbf{H}}_N)$ is the largest eigenvalue of $(\overline{\mathbf{H}}_N + \overline{\mathbf{H}}_N^\dagger)/2$ and $\rho = \|\overline{\mathbf{H}}_N\|_2$. Although tighter bounds can be found,⁴⁰ the bound given in (23) is more instructive. It shows that the approximation error made in an Arnold time integrator depends on the departure of \mathbf{V}_{kriv} from an invariant subspace of $\overline{\mathbf{H}}_N$, which is measured by β_{k+1} , the step size or time window δt as well as the spectral radius of $\overline{\mathbf{H}}_N$, measured by ρ and $\mu(\overline{\mathbf{H}}_N)$.

Unlike the Chebyshev method, where the expansion coefficients are known ahead of time, the coefficients for SIA are related to the spectrum of \mathbf{H}_{kriv} , which itself is dependent on \mathbf{v} (the current state vector, $\mathbf{m}(t)$, in the context of Eq. (12)). As such, it is canonical to adopt a dynamic time-stepping approach where the Krylov subspace dimension (k) is fixed before the simulation and each Δt_i corresponding to \mathcal{T}_i is determined dynamically throughout the time propagation. As Eq. (23) is only a loose bound, its practical ability to determine Δt is limited. Given that the Arnoldi method produces successively more accurate Krylov subspaces with increasing k , a more practical error bound is given by $c_k^{\text{kriv}}(\Delta t)$, which measures the potential for projections of the exact matrix-exponential onto vectors outside the Krylov subspace. Therefore, as has been successfully applied to the SIL method,⁴⁸ a reasonable choice for the step size is the largest Δt such that $|c_k^{\text{kriv}}(\Delta t)| < \varepsilon^{\text{krylov}}$, where $\varepsilon^{\text{krylov}} \in \mathbb{R}^+$ is a chosen error threshold.

Another side effect of the non-analytic nature of the SIA coefficients is that, unlike \mathbf{V}_{cheb} , \mathbf{V}_{kriv} must be materialized in memory and Eqs. (13) and (15) must be evaluated explicitly. As such, the memory requirement associated with SIA will grow $O(kn)$ with basis dimension. However, as will be demonstrated in Sec. 3, the SIA method will generally require fewer σ

builds than the Chebyshev method to achieve commensurate integration accuracy.

3 Results

To assess the efficacy of the Chebyshev and SIA TD-EOM-CC integrators developed in this work, we compare the accuracy and efficiency of these methods for two test systems, N_2 (1.1 Å) and MgF (1.6 Å), relative to exact dynamics (Eq. (9)) as well as RK4 and the TD-EOM-CC SIL method of Ref. 48. Each of these systems were treated at the EOM-CCSD level of theory with the minimum STO-3G basis set^{76,77} to allow for practical comparisons with exact dynamics. All ground-state CC calculations were performed using a prototype Python implementation interfaced with the HF and integral transformation routines in the PSI4 software package⁷⁸ and geometries were aligned along the z -cartesian axis without the use of point-group symmetry. At their respective geometries, both of these systems exhibit real-valued EOM-CC spectra. All simulations in this work were performed using $\epsilon^{\text{cheb}} = 10^{-16}$ and $\epsilon^{\text{krylov}} = 10^{-6}$ (for both SIL and SIA) for a duration of $\mathcal{T} = 1350 E_h^{-1}$ (≈ 32 fs).

First, we examine the temporal error accumulation in the autocorrelation function (Eq. (1)) using the normalized root-mean-square-deviation (RMSD) metric

$$E(t_j) = \sqrt{\frac{\sum_{i \leq j} |S(t_i) - S_{\text{ex}}(t_i)|^2}{\sum_{i \leq j} |S_{\text{ex}}(t_i)|^2}}, \quad t_i = i \times \delta t, \quad (24)$$

where S_{ex} is given in Eq. (11) and δt is the temporal resolution of the integrated time series. For the Chebyshev, SIA, and SIL integrators, $\delta t = 0.05 E_h^{-1}$. As the temporal resolution and step-size coincide for RK4, we have compared our methods with 3 different RK4 step-sizes to illustrate convergence: RK4-1 ($\delta t = 0.05 E_h^{-1}$), RK4-2 ($\delta t = 0.01 E_h^{-1}$), and RK4-3 ($\delta t = 0.001 E_h^{-1}$). In the following, we will use $E(\mathcal{T})$ (i.e. the total accumulated autocorrelation error) as a global error metric to assess each integrators' relative accuracy. Figure 2 illustrates the accumulated autocorrelation error for each of the integrators considered. Parameters for Chebyshev (Δt_{cheb}), SIA (k), and SIL (k) simulations in Fig. 2 were selected to

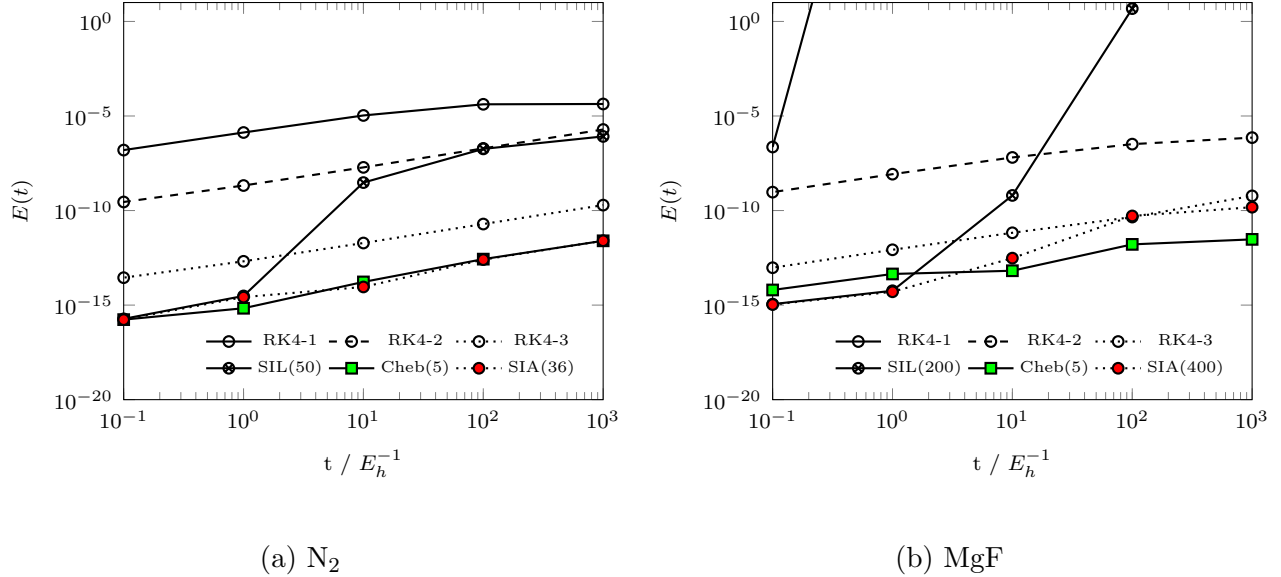


Figure 2: Accumulated $S(t)$ errors for RK4, Chebyshev, SIA, and SIL.

minimize $E(\mathcal{T})$ for each method. For N₂, the Chebyshev, SIA and RK4 integrators exhibit near constant error accumulation over the full simulation. SIL exhibits a sharp error increase between 1-10 E_h^{-1} which is of the same order as $\varepsilon^{\text{krylov}}$. For $k = 36$, SIA yields an invariant subspace up to an error of $O(\varepsilon^{\text{krylov}})$, and as such, the entire simulation ($t < \mathcal{T}$) can be performed using a single Krylov subspace. For MgF, SIL and RK4-1 diverge, while Chebyshev, SIA, RK4-2 and RK4-3 exhibit similar error accumulation characteristics as were observed for N₂. However, unlike N₂, SIA does not yield an invariant subspace even with largest subspace of $k = 400$, and thus multiple Krylov subspaces must be generated over the course of the simulation. As such, error $O(\varepsilon^{\text{krylov}})$ is compounded at each macro-time step, which explains the overtaking of SIA by Chebyshev in the long- t limit.

Figure 3 presents the cost-to-accuracy ratio, characterized by $E(\mathcal{T})$ as a function of σ builds emitted by each integrator, for a range of parameter choices. For N₂ (MgF), Chebyshev results were obtained for $\Delta t_{\text{cheb}} \in \{1, 5\}$ ($\Delta t_{\text{cheb}} \in \{1, 5, 10, 30, 50\}$). As discussed in Sec. 2.3.1, the number of required σ builds for the Chebyshev is fixed at $m_{\text{cheb}}\mathcal{T}/\Delta t_{\text{cheb}}$ and m_{cheb} generally increases as a function of Δt_{cheb} . This behaviour is shown explicitly for MgF in Fig. 4a. For both systems studied, neither $E(\mathcal{T})$ nor to the total number of

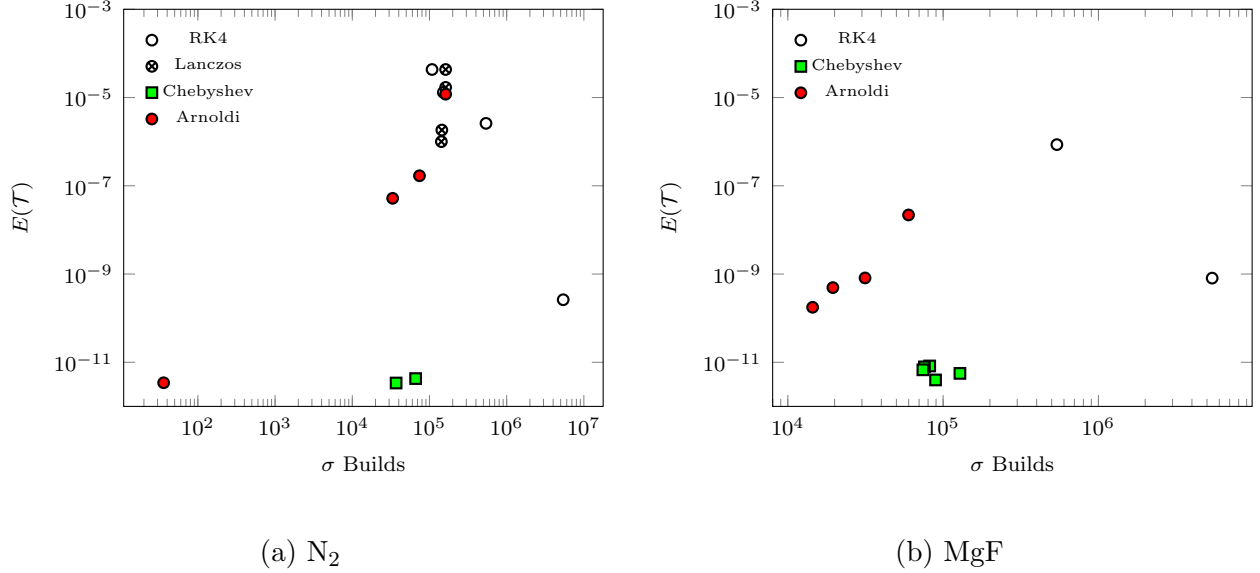


Figure 3: Cost-to-accuracy comparison for RK4, Chebyshev, SIA, and SIL.

σ -formations are significantly affected by increasing Δt_{cheb} .

SIA results were obtained for N_2 (MgF) with $k \in \{5, 10, 20, 36\}$ ($k \in \{50, 100, 200, 400\}$). As is shown in Fig. 4b, the achievable time step (σ build count) subject to $\varepsilon^{\text{krylov}}$ is (inversely) proportional to k and thus the SIA and SIL data points in Fig. 3 are plotted in order of *decreasing* k . Unlike the Chebyshev method, the accuracy of SIA consistently improves with increased k , and thus k should be maximized subject to available memory resources to improve both accuracy and efficiency of the SIA method.

For N_2 , SIL results were also obtained with $k \in \{5, 10, 20, 36, 50\}$ for a direct order-by-order comparison with SIA. At each order, SIA achieves between 2-3 orders of magnitude better accuracy over SIL, and requires $>50\%$ fewer σ builds in cases where SIA is able to take time-steps larger than δt ($k \geq 10$). This is due to the fact that the Arnoldi method generates a faithful Krylov subspace representation $\overline{\mathbf{H}}_N$ while the Lanczos method, being only valid for Hermitian matrices, does not. This fact is particularly apparent in SIA's generation of an invariant subspace for $k = 36$ while SIL fails to demonstrate similar convergence.

For all problems considered, the proposed SIA and Chebyshev integrators exhibit superior accuracy and efficiency over analogous SIL and RK4 simulations. While it is possible for RK4

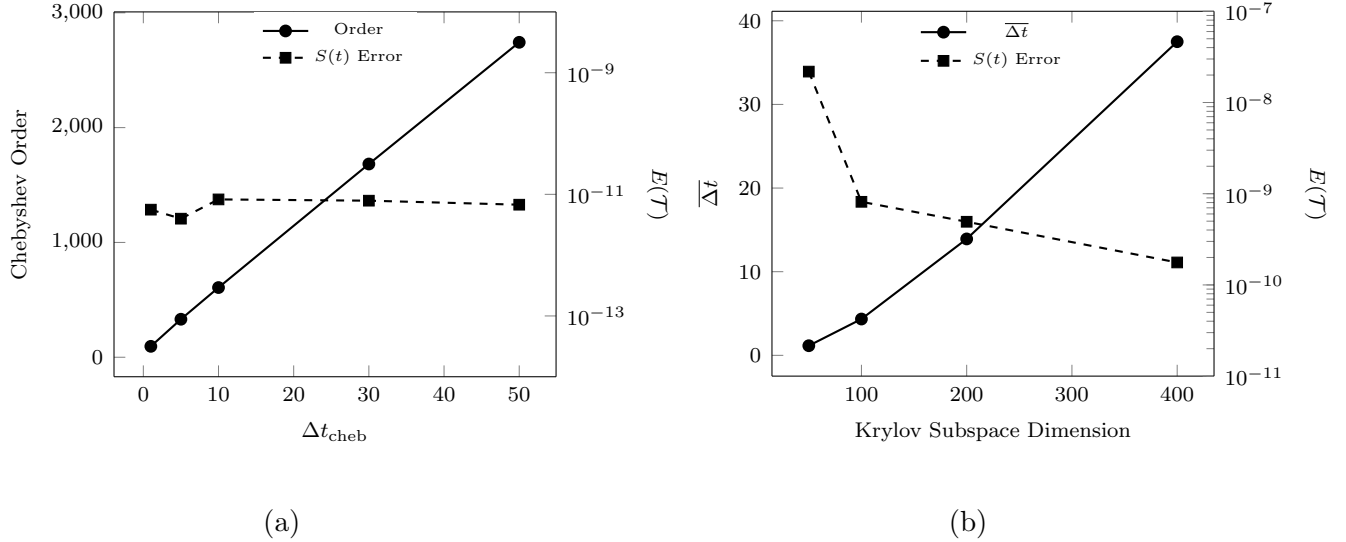


Figure 4: Assessment of the variance of cost and accuracy of (a) Chebyshev and (b) SIA integrators as a function of parameter selection. SIA results are presented as the average time-step $\overline{\Delta t}$ as a function of k .

to yield reasonable accuracy at small time-steps (RK4-3), these simulations require excessive number of σ builds and would not be practical for the simulation of realistic TD-EOM-CC problems.

4 Conclusions

In this work, we have presented two approximate exponential time-integrators for TD-EOM-CC theory based on Chebyshev and Arnoldi (SIA) expansions of the quantum propagator. The efficacies of these integrators were demonstrated via comparison with exact exponential dynamics for two small test problems. The Chebyshev and SIA integrators were demonstrated to yield superior accuracy and efficiency when compared to RK4 and the recently developed SIL method for TD-EOM-CC.⁴⁸ As both of the presented methods are built from standard algorithmic components required for any implementation of (TD-)EOM-CC, the implementation of these methods has a low barrier for entry and holds the potential to yield significant performance and accurate improvements for these simulations in the future.

The practical application of the presented schemes requires consideration of the balance

between desired integration accuracy and available computational resources. If memory capacity allows, the SIA method would be preferred for most chemistry applications due to its systematic improvability with respect to truncation order. However, the memory requirement of SIA quickly becomes prohibitive for large problems and the explicit orthogonalization requirement complicated efficient distributed memory implementations. In these instances, the Chebyshev method would be preferred due to its low memory requirement and the simplicity of its implementation.

While the results presented in this work have focused on the moment-based formalism of TD-EOM-CC, the presented efficacy experiments serve as an important proof-of-concept to demonstrate the the proposed methods for general TD-EOM-CC simulations. Future work to extend these methods to large scale TD-EOM-CC simulations is currently being pursued by the authors. Further, extension of these methods for use with time-dependent Hamiltonians, such as those required to study field-driven dynamics of molecular systems, are currently under development.

Acknowledgement

This material is based upon work supported by the U.S. Department of Energy, Office of Science, Office of Advanced Scientific Computing Research and Office of Basic Energy Sciences, Scientific Discovery through the Advanced Computing (SciDAC) program under Award No. DE-SC0022263. This project used resources of the National Energy Research Scientific Computing Center, a DOE Office of Science User Facility supported by the Office of Science of the U.S. Department of Energy under Contract No. DE-AC02-05CH11231 using NERSC award ERCAP-0024336.

References

- (1) Goings, J. J.; Lestrangle, P. J.; Li, X. Real-time time-dependent electronic structure theory. *WIREs Computational Molecular Science* **2018**, *8*, e1341.
- (2) Li, X.; Govind, N.; Isborn, C.; DePrince, A. E. I.; Lopata, K. Real-Time Time-Dependent Electronic Structure Theory. *Chemical Reviews* **2020**, *120*, 9951–9993.
- (3) Dreuw, A.; Head-Gordon, M. Single-Reference ab Initio Methods for the Calculation of Excited States of Large Molecules. *Chemical Reviews* **2005**, *105*, 4009–4037.
- (4) Olsen, J.; Jørgensen, P. Linear and nonlinear response functions for an exact state and for an MCSCF state. *The Journal of Chemical Physics* **1985**, *82*, 3235–3264.
- (5) Datta, B.; Sen, P.; Mukherjee, D. Coupled-Cluster Based Linear Response Approach to Property Calculations: Dynamic Polarizability and Its Static Limit. *The Journal of Physical Chemistry* **1995**, *99*, 6441–6451.
- (6) Oddershede, J.; Jørgensen, P.; Yeager, D. L. Polarization propagator methods in atomic and molecular calculations. *Computer Physics Reports* **1984**, *2*, 33–92.
- (7) Linderberg, J.; Öhrn, Y. *Propagators in quantum chemistry*; John Wiley & Sons, 2004.
- (8) Norman, P. A perspective on nonresonant and resonant electronic response theory for time-dependent molecular properties. *Phys. Chem. Chem. Phys.* **2011**, *13*, 20519–20535.
- (9) Ring, P.; Schuck, P. *The nuclear many-body problem*; Springer Science & Business Media, 2004.
- (10) Shavitt, I.; Bartlett, R. J. *Many-body methods in chemistry and physics: MBPT and coupled-cluster theory*; Cambridge university press, 2009.

- (11) Stanton, J. F.; Bartlett, R. J. The equation of motion coupled-cluster method. A systematic biorthogonal approach to molecular excitation energies, transition probabilities, and excited state properties. *The Journal of Chemical Physics* **1993**, *98*, 7029–7039.
- (12) Rico, R. J.; Head-Gordon, M. Single-reference theories of molecular excited states with single and double substitutions. *Chemical Physics Letters* **1993**, *213*, 224–232.
- (13) Trofimov, A.; Krivdina, I.; Weller, J.; Schirmer, J. Algebraic-diagrammatic construction propagator approach to molecular response properties. *Chemical Physics* **2006**, *329*, 1–10, Electron Correlation and Multimode Dynamics in Molecules.
- (14) Dreuw, A.; Dempwolff, A. L. In *Theoretical and Computational Photochemistry*; García-Iriepa, C., Marazzi, M., Eds.; Elsevier, 2023; pp 119–134.
- (15) Peng, B.; Bauman, N. P.; Gulania, S.; Kowalski, K. In *Chapter Two - Coupled cluster Green's function: Past, present, and future*; Dixon, D. A., Ed.; Annual Reports in Computational Chemistry; Elsevier, 2021; Vol. 17; pp 23–53.
- (16) Cederbaum, L.; Zobeley, J. Ultrafast charge migration by electron correlation. *Chemical Physics Letters* **1999**, *307*, 205–210.
- (17) Coriani, S.; Høst, S.; Jansík, B.; Thøgersen, L.; Olsen, J.; Jørgensen, P.; Reine, S.; Pawłowski, F.; Helgaker, T.; Salek, P. Linear-scaling implementation of molecular response theory in self-consistent field electronic-structure theory. *The Journal of Chemical Physics* **2007**, *126*, 154108.
- (18) Kauczor, J.; Jørgensen, P.; Norman, P. On the Efficiency of Algorithms for Solving Hartree–Fock and Kohn–Sham Response Equations. *Journal of Chemical Theory and Computation* **2011**, *7*, 1610–1630.
- (19) Coriani, S.; Fransson, T.; Christiansen, O.; Norman, P. Asymmetric-Lanczos-Chain-

- Driven Implementation of Electronic Resonance Convergent Coupled-Cluster Linear Response Theory. *Journal of Chemical Theory and Computation* **2012**, *8*, 1616–1628.
- (20) Kauczor, J.; Norman, P.; Christiansen, O.; Coriani, S. Communication: A reduced-space algorithm for the solution of the complex linear response equations used in coupled cluster damped response theory. *The Journal of Chemical Physics* **2013**, *139*, 211102.
- (21) Van Beeumen, R.; Williams-Young, D. B.; Kasper, J. M.; Yang, C.; Ng, E. G.; Li, X. Model Order Reduction Algorithm for Estimating the Absorption Spectrum. *Journal of Chemical Theory and Computation* **2017**, *13*, 4950–4961.
- (22) Peng, B.; Van Beeumen, R.; Williams-Young, D. B.; Kowalski, K.; Yang, C. Approximate Green’s Function Coupled Cluster Method Employing Effective Dimension Reduction. *Journal of Chemical Theory and Computation* **2019**, *15*, 3185–3196.
- (23) Micha, D. A.; Runge, K. Time-dependent many-electron approach to slow ion-atom collisions: The coupling of electronic and nuclear motions. *Phys. Rev. A* **1994**, *50*, 322–336.
- (24) Li, X.; Smith, S. M.; Markevitch, A. N.; Romanov, D. A.; Levis, R. J.; Schlegel, H. B. A time-dependent Hartree–Fock approach for studying the electronic optical response of molecules in intense fields. *Phys. Chem. Chem. Phys.* **2005**, *7*, 233–239.
- (25) Isborn, C. M.; Li, X.; Tully, J. C. Time-dependent density functional theory Ehrenfest dynamics: Collisions between atomic oxygen and graphite clusters. *The Journal of Chemical Physics* **2007**, *126*, 134307.
- (26) Krause, P.; Klamroth, T.; Saalfrank, P. Time-dependent configuration-interaction calculations of laser-pulse-driven many-electron dynamics: Controlled dipole switching in lithium cyanide. *The Journal of Chemical Physics* **2005**, *123*, 074105.

- (27) Schlegel, H. B.; Smith, S. M.; Li, X. Electronic optical response of molecules in intense fields: Comparison of TD-HF, TD-CIS, and TD-CIS(D) approaches. *The Journal of Chemical Physics* **2007**, *126*, 244110.
- (28) Lestrange, P. J.; Hoffmann, M. R.; Li, X. In *Novel Electronic Structure Theory: General Innovations and Strongly Correlated Systems*; Hoggan, P. E., Ed.; Advances in Quantum Chemistry; Academic Press, 2018; Vol. 76; pp 295–313.
- (29) Sonk, J. A.; Caricato, M.; Schlegel, H. B. TD-CI Simulation of the Electronic Optical Response of Molecules in Intense Fields: Comparison of RPA, CIS, CIS(D), and EOM-CCSD. *The Journal of Physical Chemistry A* **2011**, *115*, 4678–4690.
- (30) Leforestier, C.; Bisseling, R.; Cerjan, C.; Feit, M.; Friesner, R.; Guldberg, A.; Hammerich, A.; Jolicard, G.; Karrlein, W.; Meyer, H.-D.; Lipkin, N.; Roncero, O.; Kosloff, R. A comparison of different propagation schemes for the time dependent Schrödinger equation. *Journal of Computational Physics* **1991**, *94*, 59–80.
- (31) Gómez Pueyo, A.; Marques, M. A. L.; Rubio, A.; Castro, A. Propagators for the Time-Dependent Kohn–Sham Equations: Multistep, Runge–Kutta, Exponential Runge–Kutta, and Commutator Free Magnus Methods. *Journal of Chemical Theory and Computation* **2018**, *14*, 3040–3052.
- (32) Tal-Ezer, H.; Kosloff, R. An accurate and efficient scheme for propagating the time dependent Schrödinger equation. *The Journal of Chemical Physics* **1984**, *81*, 3967–3971.
- (33) Williams-Young, D.; Goings, J. J.; Li, X. Accelerating Real-Time Time-Dependent Density Functional Theory with a Nonrecursive Chebyshev Expansion of the Quantum Propagator. *Journal of Chemical Theory and Computation* **2016**, *12*, 5333–5338, PMID: 27749071.

- (34) Baer, R.; Neuhauser, D. Real-time linear response for time-dependent density-functional theory. *The Journal of Chemical Physics* **2004**, *121*, 9803–9807.
- (35) Wang, F.; Yam, C. Y.; Chen, G.; Fan, K. Density matrix based time-dependent density functional theory and the solution of its linear response in real time domain. *The Journal of Chemical Physics* **2007**, *126*, 134104.
- (36) Park, T. J.; Light, J. C. Unitary quantum time evolution by iterative Lanczos reduction. *The Journal of Chemical Physics* **1986**, *85*, 5870–5876.
- (37) Hairer, E.; Hochbruck, M.; Iserles, A.; Lubich, C. Geometric numerical integration. *Oberwolfach Reports* **2006**, *3*, 805–882.
- (38) Saad, Y. Analysis of Some Krylov Subspace Approximations to the Matrix Exponential Operator. *SIAM Journal on Numerical Analysis* **1992**, *29*, 209–228.
- (39) Al-Mohy, A. H.; Higham, N. J. Computing the Action of the Matrix Exponential, with an Application to Exponential Integrators. *SIAM Journal on Scientific Computing* **2011**, *33*, 488–511.
- (40) Hochbruck, M.; Lubich, C. On Krylov Subspace Approximations to the Matrix Exponential Operator. *SIAM Journal on Numerical Analysis* **1997**, *34*, 1911–1925.
- (41) Sverdrup Ofstad, B.; Aurbakken, E.; Sigmundson Schøyen, Ø.; Kristiansen, H. E.; Kvaal, S.; Pedersen, T. B. Time-dependent coupled-cluster theory. *WIREs Computational Molecular Science* **2023**, *n/a*, e1666.
- (42) Gray, S. K.; Manolopoulos, D. E. Symplectic integrators tailored to the time-dependent Schrödinger equation. *The Journal of Chemical Physics* **1996**, *104*, 7099–7112.
- (43) Park, Y. C.; Perera, A.; Bartlett, R. J. Equation of motion coupled-cluster for core excitation spectra: Two complementary approaches. *The Journal of Chemical Physics* **2019**, *151*, 164117.

- (44) Pedersen, T. B.; Kvaal, S. Symplectic integration and physical interpretation of time-dependent coupled-cluster theory. *The Journal of Chemical Physics* **2019**, *150*, 144106.
- (45) Pathak, H.; Panyala, A.; Peng, B.; Bauman, N. P.; Mutlu, E.; Rehr, J. J.; Vila, F. D.; Kowalski, K. Real-Time Equation-of-Motion Coupled-Cluster Cumulant Green's Function Method: Heterogeneous Parallel Implementation Based on the Tensor Algebra for Many-Body Methods Infrastructure. *Journal of Chemical Theory and Computation* **2023**, *19*, 2248–2257, PMID: 37096369.
- (46) Wang, Z.; Peyton, B. G.; Crawford, T. D. Accelerating Real-Time Coupled Cluster Methods with Single-Precision Arithmetic and Adaptive Numerical Integration. *Journal of Chemical Theory and Computation* **2022**, *18*, 5479–5491, PMID: 35939815.
- (47) Sato, T.; Pathak, H.; Orimo, Y.; Ishikawa, K. L. Communication: Time-dependent optimized coupled-cluster method for multielectron dynamics. *The Journal of Chemical Physics* **2018**, *148*, 051101.
- (48) Cooper, B. C.; Koulias, L. N.; Nascimento, D. R.; Li, X.; DePrince, A. E. I. Short Iterative Lanczos Integration in Time-Dependent Equation-of-Motion Coupled-Cluster Theory. *The Journal of Physical Chemistry A* **2021**, *125*, 5438–5447.
- (49) Luppi, E.; Head-Gordon, M. Computation of high-harmonic generation spectra of H₂ and N₂ in intense laser pulses using quantum chemistry methods and time-dependent density functional theory. *Molecular Physics* **2012**, *110*, 909–923.
- (50) Skeidsvoll, A. S.; Moitra, T.; Balbi, A.; Paul, A. C.; Coriani, S.; Koch, H. Simulating weak-field attosecond processes with a Lanczos reduced basis approach to time-dependent equation-of-motion coupled-cluster theory. *Phys. Rev. A* **2022**, *105*, 023103.
- (51) Nascimento, D. R.; DePrince, A. E. I. Linear Absorption Spectra from Explicitly Time-Dependent Equation-of-Motion Coupled-Cluster Theory. *Journal of Chemical Theory and Computation* **2016**, *12*, 5834–5840.

- (52) Nascimento, D. R.; DePrince, I., A. Eugene A general time-domain formulation of equation-of-motion coupled-cluster theory for linear spectroscopy. *The Journal of Chemical Physics* **2019**, *151*, 204107.
- (53) Moler, C.; Van Loan, C. Nineteen Dubious Ways to Compute the Exponential of a Matrix, Twenty-Five Years Later. *SIAM Review* **2003**, *45*, 3–49.
- (54) Yuwono, S. H.; Cooper, B. C.; Zhang, T.; Li, X.; DePrince III, A. E. Time-Dependent Equation-of-Motion Coupled-Cluster Simulations with a Defective Hamiltonian. *J. Chem. Phys.* **2023**, *159*, 044113.
- (55) Kjønstad, E. F.; Myhre, R. H.; Martínez, T. J.; Koch, H. Crossing conditions in coupled cluster theory. *The Journal of Chemical Physics* **2017**, *147*, 164105.
- (56) Thomas, S.; Hampe, F.; Stopkowicz, S.; Gauss, J. Complex ground-state and excitation energies in coupled-cluster theory. *Molecular Physics* **2021**, *119*, e1968056.
- (57) Burden, R. L.; Faires, J. D.; Burden, A. M. *Numerical analysis*; Cengage learning, 2015.
- (58) Sorensen, D. C. In *Parallel Numerical Algorithms*; Keyes, D. E., Sameh, A., Venkatakrishnan, V., Eds.; Springer Netherlands: Dordrecht, 1997; pp 119–165.
- (59) Lehoucq, R. B.; Sorensen, D. C.; Yang, C. *ARPACK users' guide: solution of large-scale eigenvalue problems with implicitly restarted Arnoldi methods*; SIAM, 1998.
- (60) Kjønstad, E. F.; Folkestad, S. D.; Koch, H. Accelerated multimodel Newton-type algorithms for faster convergence of ground and excited state coupled cluster equations. *The Journal of Chemical Physics* **2020**, *153*, 014104.
- (61) Zuev, D.; Vecharynski, E.; Yang, C.; Orms, N.; Krylov, A. I. New algorithms for iterative matrix-free eigensolvers in quantum chemistry. *Journal of Computational Chemistry* **2015**, *36*, 273–284.

- (62) Caricato, M.; Trucks, G. W.; Frisch, M. J. A Comparison of Three Variants of the Generalized Davidson Algorithm for the Partial Diagonalization of Large Non-Hermitian Matrices. *Journal of Chemical Theory and Computation* **2010**, *6*, 1966–1970, PMID: 26615925.
- (63) Bader, P.; Blanes, S.; Casas, F.; Seydaoğlu, M. An efficient algorithm to compute the exponential of skew-Hermitian matrices for the time integration of the Schrödinger equation. *Mathematics and Computers in Simulation* **2022**, *194*, 383–400.
- (64) Lubich, C. *From Quantum to Classical Molecular Dynamics: Reduced Models and Numerical Analysis*; EMS Press, 2008.
- (65) Stewart, G. W. *Matrix Algorithms: Volume II: Eigensystems*; SIAM, 2001.
- (66) Saad, Y. *Numerical methods for large eigenvalue problems: revised edition*; SIAM, 2011.
- (67) Paige, C. Error analysis of the Lanczos algorithm for tridiagonalizing a symmetric matrix. *J. Inst. Math. Appl.* **1976**, *18*, 341–349.
- (68) Parlett, B. N.; Scott, D. S. The Lanczos Algorithm with Selective Orthogonalization. *Mathematics of Computation* **1979**, *33*, 217–238.
- (69) Simon, H. D. Analysis of the symmetric Lanczos algorithm with reorthogonalization methods. *Linear Algebra and its Applications* **1984**, *61*, 101–131.
- (70) Daniel, J.; Gragg, W.; Kaufman, L.; Stewart, G. Reorthogonalization and stable algorithms for updating the Gram-Schmidt QR factorization. *Math. Comp.* **1976**, *30*, 772–795.
- (71) Saad, Y. The Lanczos Biorthogonalization Algorithm and Other Oblique Projection Methods for Solving Large Unsymmetric Systems. *SIAM Journal on Numerical Analysis* **1982**, *19*, 485–506.

- (72) Parlett, B. N.; Taylor, D. R.; Liu, Z. A. A Look-Ahead Lanczos Algorithm for Unsymmetric Matrices. *Mathematics of Computation* **1985**, *44*, 105–124.
- (73) Gutknecht, M. H. A Completed Theory of the Unsymmetric Lanczos Process and Related Algorithms, Part I. *SIAM Journal on Matrix Analysis and Applications* **1992**, *13*, 594–639.
- (74) van der Veen, H.; Vuik, K. Bi-Lanczos with partial orthogonalization. *Computers & Structures* **1995**, *56*, 605–613.
- (75) Arioli, M.; Fassino, C. Roundoff error analysis of algorithms based on Krylov subspace methods. *Bit Numer Math* **1996**, *36*, 189–205.
- (76) Hehre, W. J.; Stewart, R. F.; Pople, J. A. Self-Consistent Molecular-Orbital Methods. I. Use of Gaussian Expansions of Slater-Type Atomic Orbitals. *J. Chem. Phys.* **1969**, *51*, 2657–2664.
- (77) Hehre, W. J.; Ditchfield, R.; Stewart, R. F.; Pople, J. A. Self-Consistent Molecular Orbital Methods. IV. Use of Gaussian Expansions of Slater-Type Orbitals. Extension to Second-Row Molecules. *J. Chem. Phys.* **1970**, *52*, 2769–2773.
- (78) Smith, D. G. A.; Burns, L. A.; Simmonett, A. C.; Parrish, R. M.; Schieber, M. C.; Galvelis, R.; Kraus, P.; Kruse, H.; Di Remigio, R.; Alenaizan, A.; James, A. M.; Lehtola, S.; Misiewicz, J. P.; Scheurer, M.; Shaw, R. A.; Schriber, J. B.; Xie, Y.; Glick, Z. L.; Sirianni, D. A.; O’Brien, J. S.; Waldrop, J. M.; Kumar, A.; Hohenstein, E. G.; Pritchard, B. P.; Brooks, B. R.; Schaefer, H. F.; Sokolov, A. Y.; Patkowski, K.; DePrince, A. E.; Bozkaya, U.; King, R. A.; Evangelista, F. A.; Turney, J. M.; Crawford, T. D.; Sherrill, C. D. PSI4 1.4: Open-source software for high-throughput quantum chemistry. *J. Chem. Phys.* **2020**, *152*, 184108.